Chronic partial TrkB activation reduces seizures and mortality in a mouse model of Dravet syndrome

Feng Gu[a] , Isabel Parada[a], Tao Yang[a] , Frank M. Longo[a], and David A. Prince[a,1]

[a]Department of Neurology & Neurological Sciences, Stanford University School of Medicine, Stanford, CA 94305-5122

Dravet syndrome (DS) is one of the most severe childhood epilepsies, characterized by intractable seizures and comorbidities including cognitive and social dysfunction and high premature mortality. DS is mainly caused by loss-of-function mutations in the *Scn1a* gene encoding $Na_v1.1$ that is predominantly expressed in inhibitory parvalbumin-containing (PV) interneurons. Decreased $Na_v1.1$ impairs PV cell function, contributing to DS phenotypes. Effective pharmacological therapy that targets defective PV interneurons is not available. The known role of brain-derived neurotrophic factor (BDNF) in the development and maintenance of interneurons, together with our previous results showing improved PV interneuronal function and antiepileptogenic effects of a TrkB receptor agonist in a posttraumatic epilepsy model, led to the hypothesis that early treatment with a TrkB receptor agonist might prevent or reduce seizure activity in DS mice. To test this hypothesis, we treated DS mice with LM22A-4 (LM), a partial agonist at the BDNF TrkB receptor, for 7 d starting at postnatal day 13 (P13), before the onset of spontaneous seizures. Results from immunohistochemistry, Western blot, whole-cell patch-clamp recording, and in vivo seizure monitoring showed that LM treatment increased the number of perisomatic PV interneuronal synapses around cortical pyramidal cells in layer V, upregulated $Na_v1.1$ in PV neurons, increased inhibitory synaptic transmission, and decreased seizures and the mortality rate in DS mice. The results suggest that early treatment with a partial TrkB receptor agonist may be a promising therapeutic approach to enhance PV interneuron function and reduce epileptogenesis and premature death in DS.

epilepsy | Dravet syndrome | TrkB | interneuron

Dravet syndrome (DS), also known as severe myoclonic epilepsy of infancy, is one of the most severe childhood epilepsies, characterized by intractable frequent seizures, cognitive and social dysfunction, ataxia, and high premature mortality (1, 2). Although recent drug trials have shown some effects on reducing convulsive seizure frequency (3–5), additional therapeutic approaches are still in great need to better control seizures and improve cognitive and other behavioral deficits as well as survival in children suffering from this devastating disease. Parvalbumin-containing (PV) interneurons play a critical role in controlling the activity of excitatory cells in brain circuits and in sensory processing, rhythm generation, and cognition. Abnormalities in PV interneurons contribute to a variety of neurological disorders, including DS. In most cases, DS is caused by loss-of-function mutations in the *Scn1a* gene that encodes the α-subunit of the voltage-gated sodium channel $Na_v1.1$ (6). Because $Na_v1.1$ is mainly expressed in axon initial segments (AIS) and somata of interneurons, especially PV cells in the brain (7), the loss of $Na_v1.1$ impairs the action potential firing of those cells and decreases inhibitory GABAergic neurotransmission, contributing to excessive activity in excitatory networks, seizures, and other behavioral deficits in DS mice (6–9). The characteristic fast-firing pattern of PV interneurons is particularly affected, as indicated by increased rheobase and threshold and decreased amplitude and frequency of action potential firing in response to depolarizing current injection (7, 10). Specific inactivation of $Na_v1.1$ from PV interneurons leads to spontaneous

seizures, cognitive dysfunction, and social deficits (11–13), further supporting the important role of dysfunctional PV cells in the pathophysiology of DS. Results in patients and animal models of DS have suggested that treatment with GABAergic drugs may result in a modest improvement in seizures and behavioral abnormalities (9, 14). The important role of PV interneurons in the pathogenesis of DS suggests that approaches to increase GABAergic inhibition from these cells may offer a potential strategy for treatment. Therapy that targets defective PV interneurons is currently not available. The known role of brain-derived neurotrophic factor (BDNF) in the development and maintenance of interneurons, together with our previous results showing improved function of PV interneurons and antiepileptogenic effects of TrkB receptor activation in a model of posttraumatic epilepsy (15), lead to the hypothesis that early treatment with a small-molecule TrkB receptor agonist may prevent or reduce seizures and death in DS mice by enhancing PV interneuron function.

To test this hypothesis, we treated postnatal day 13 (P13) DS mice with saline or LM22A-4 (LM), starting at P13 before the onset of spontaneous seizures. LM is a small-molecule partial TrkB receptor agonist with its structure similar to loop II of BDNF (16), a region that confers TrkB activation and specificity (17). LM can cross the blood–brain barrier to specifically activate TrkB and its associated downstream AKT and ERK

Significance

Dravet syndrome (DS) is a severe childhood epileptic encephalopathy characterized by intractable seizures and comorbidities, including a high rate of premature mortality. DS is mainly caused by loss-of-function mutations of the *Scn1a* gene encoding sodium channel $Na_v1.1$ that is predominantly expressed in inhibitory parvalbumin-containing (PV) interneurons. Decreased $Na_v1.1$ impairs PV cell function, causing DS phenotypes. Effective pharmacological therapy targeting defective PV interneurons is currently not available. This study demonstrated that early treatment with a partial TrkB receptor agonist, LM22A-4, increased $Na_v1.1$ expression, improved PV interneuron function, and reduced seizure occurrence and mortality rate in DS mice, suggesting a potential therapy for DS.

NEUROSCIENCE

signaling (16) and has favorable effects in rodent models of Huntington's disease, posttraumatic epilepsy, stroke, and Rett syndrome (15, 16, 18–20). In the present study, immunohistochemistry (IHC) was used to assess the density of $Na_v1.1$-immunoreactivity (IR) and colocalized PV/synaptotagmin 2/NeuN-IR (presumptive inhibitory synapses) around layer V neocortical pyramidal (Pyr) cell somata. Whole-cell recordings of inhibitory postsynaptic currents (IPSCs) were obtained from layer V Pyr cells to evaluate inhibitory synaptic transmission. The incidence of spontaneous seizures was assessed blindly in saline- and LM-treated DS mice that were monitored from P21 to P23, 2 d after the last dose of LM. Results showed that LM treatment increased the density of perisomatic PV interneuronal synapses around cortical Pyr cells in layer V, upregulated $Na_v1.1$ in PV interneurons, increased the frequency of miniature IPSCs (mIPSCs) and spontaneous IPSCs (sIPSCs), and decreased the incidence and frequency of spontaneous seizures and mortality rate in DS mice. Results suggest that chronic TrkB activation with a partial agonist may be a promising strategy to enhance PV interneuron function and thereby suppress epilepsy, mortality, and potentially other associated phenotypes, such as cognitive and social deficits in DS.

Results

LM Treatment Increases PV Synapses on the Somata of Neocortical Pyr Cells in DS Mice.
Previous results showed that the small-molecule TrkB partial agonist LM increased the number of PV inhibitory synapses on the somata of layer Va Pyr cells in an injured as well as uninjured neocortex (15). To investigate whether LM treatment can similarly enhance the PV synapses on the somata of neocortical Pyr cells in DS mice, we processed tissue sections from the cortex of mice that had been treated in vivo with saline or LM. IHC and confocal microscopy were used to assess the density of colocalized PV/synaptotagmin-2/

NeuN-IR around the somata of layer Va Pyr cells (21) (Fig. 1). Confocal images from saline-treated and LM-treated DS mice (Fig. 1 C and D) showed that the density of colocalized PV/synaptotagmin-2/NeuN-IR (presumptive inhibitory PV synapses) in the perisomatic region of interest (ROI) was significantly increased in the LM-treated (15.30 ± 0.42%, n = 9 sections from 4 mice) vs. saline-treated group (2.29 ± 0.16%, n = 9 sections from 4 mice, P < 0.01 by post hoc Tukey's test following one-way ANOVA) (Fig. 1E), indicating that chronic treatment with the partial TrkB agonist increased the density of PV interneuron synapses in the cortex of DS mice. A similar increase of PV synapse density was also found in LM-treated wild-type (WT) mice (16.13 ± 0.70%, n = 8 sections from 4 mice) vs. saline-treated WT mice (5.39 ± 0.33%, n = 8 sections from 4 mice, P < 0.01 by post hoc Tukey's test following one-way ANOVA) (Fig. 1 A, B, and E).

To confirm the effects of LM on PV synapses, additional IHC experiments and analyses were performed to measure the density of colocalized vesicular GABA transporter (VGAT)/PV/gephyrin-IR in the perisomatic ROI of layer Va Pyr cells (*SI Appendix*, Fig. S1). Results showed a similar increase of VGAT/PV/gephyrin colocalization in LM-treated vs. saline-treated mice, further suggesting that LM treatment increased the density of PV interneuron synapses on layer Va Pyr neurons.

LM Treatment Enhances Inhibitory Synaptic Transmission in DS Mice.
To investigate the effect of LM treatment on the function of PV interneurons in DS mice, we obtained whole-cell patch-clamp recordings of mIPSCs and sIPSCs from layer Va Pyr cells to evaluate inhibitory synaptic transmission. Consistent with the increased number of PV synapses indicated by the IHC results, electrophysiological recordings showed that the frequency of mIPSCs is higher in LM-treated (14.06 ± 1.96 Hz, n = 11 cells from 5 mice) vs. saline-treated DS mice (8.80 ± 0.59 Hz, n = 14
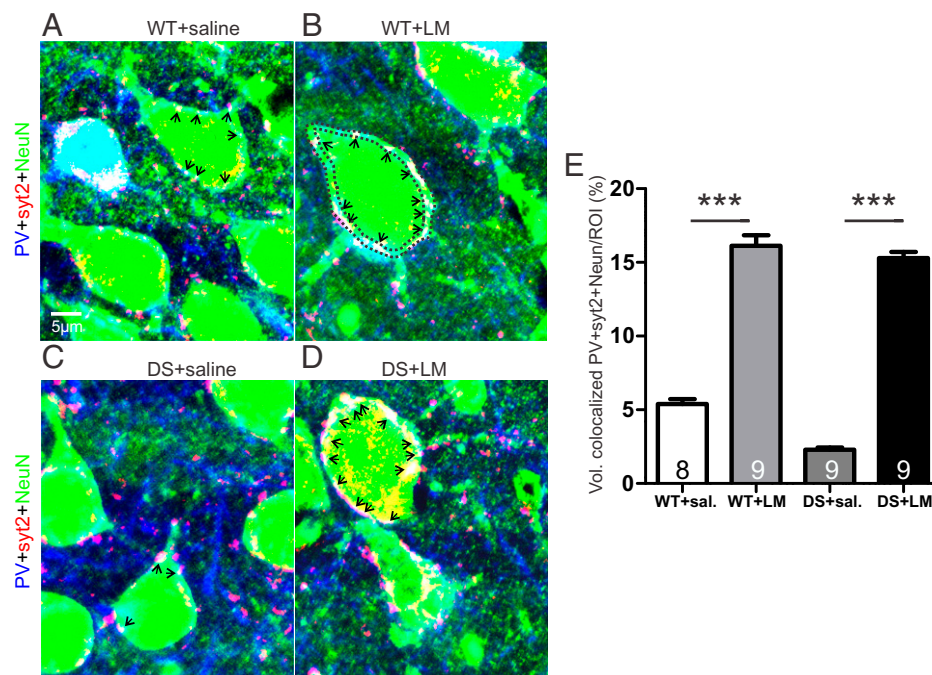
Fig. 1. LM treatment increases PV synapses on somata of Pyr cells in the cortex of DS mice. (*A–D*) Confocal images of triple IR for PV (blue)+synaptotagmin-2 (syt2; red)+NeuN (green) from layer Va of sections from saline-treated WT (*A*) and DS (*C*) mice and LM-treated WT (*B*) and DS (*D*) mice. Arrows point to perisomatic sites of colocalization of PV/syt2/NeuN-IR (white; presumptive PV synapses). "Railroad track" (black dash lines) around the soma of a Pyr cell in *B* indicates perisomatic ROI. (*E*) The graph shows a significant increase in the colocalization of PV/syt2/NeuN-IR in perisomatic ROI in LM- vs. saline (sal)-treated WT and DS mice. Results are expressed as the cumulative volume of colocalized IR/total volume of perisomatic ROI. Numbers in bars: number of sections. ***P < 0.01 by post hoc Tukey's test following one-way ANOVA (P < 0.0001, F = 238.1).

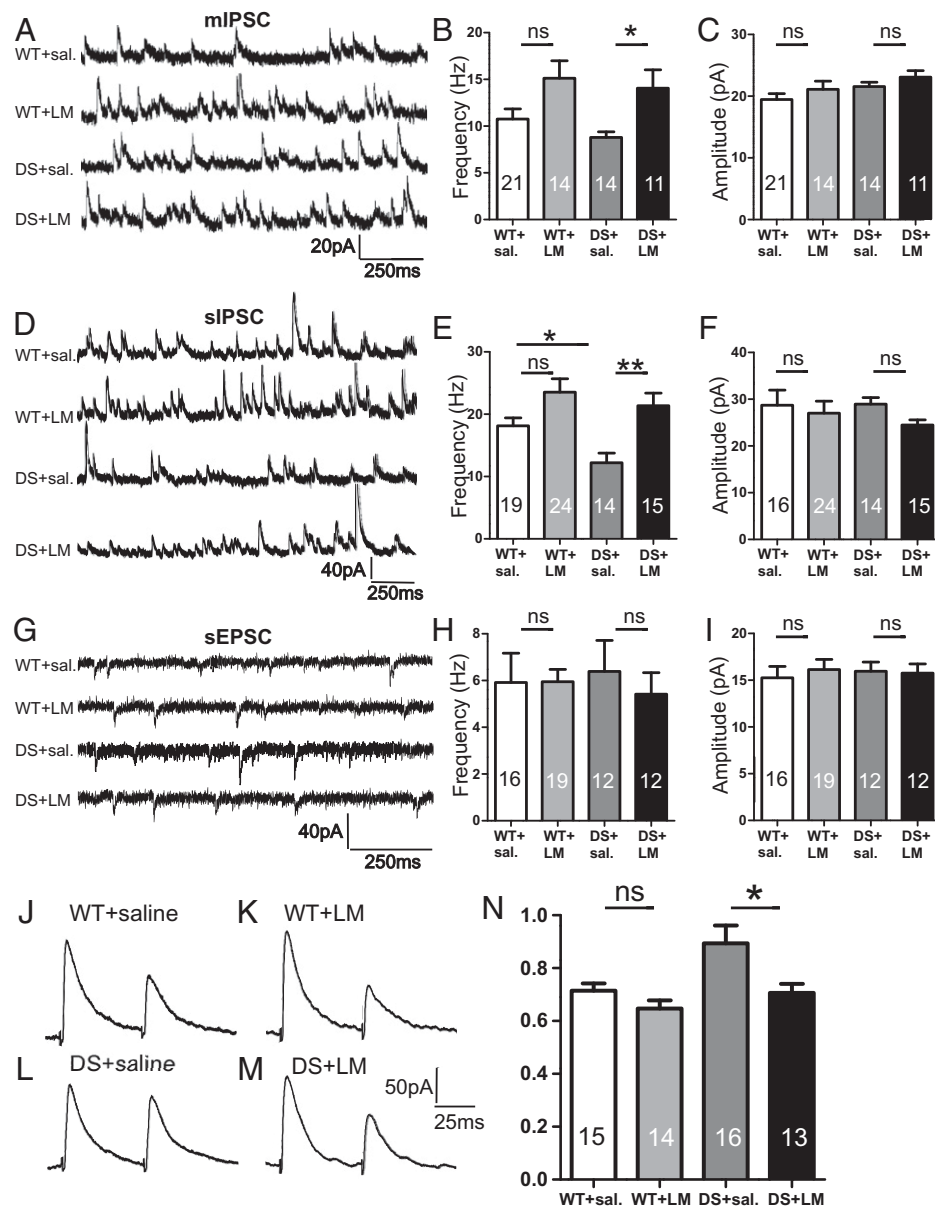**Fig. 2.** LM treatment of DS mice increases inhibitory synaptic transmission in the cortex. (*A* and *D*) Representative traces of mIPSCs (*A*) and sIPSCs (*D*) recorded from layer Va Pyr cells in the cortex of saline (sal)-treated and LM-treated WT and DS mice. (*B*, *C*, *E*, and *F*) Graphs show a significant increase in the frequency of mIPSCs (*B*) and sIPSCs (*E*) in DS mice treated with LM vs. saline, with no significant change in the amplitude (*C* and *F*). Numbers in bars: number of cells. *$P < 0.05$; **$P < 0.01$ by post hoc Tukey's test following one-way ANOVA. (*B*) $P = 0.0096$, F = 4.18; (*E*) $P = 0.0008$, F = 6.30. (*G*) Representative traces of sEPSCs. (*H* and *I*) Graphs show no significant differences in the frequency (*H*) and amplitude (*I*) of sEPSCs between saline- and LM-treated WT and DS mice. (*J–M*) Representative monosynaptic IPSCs evoked in layer Va Pyr cells by paired electrical stimuli in saline-treated (*J* and *L*) and LM-treated (*K* and *M*) WT and DS mice. (*N*) Mean PPR for eIPSCs in LM-treated DS mice is significantly decreased compared with that in saline-treated DS mice. Numbers in bars: number of cells. *$P < 0.05$ by post hoc Dunn's test following the Kruskal–Wallis test. ns, not significant.

cells from 5 mice; *$P < 0.05$ by post hoc Tukey's test following one-way ANOVA), with no significant change in amplitude (Fig. 2 *A–C*). The frequency of sIPSCs was also increased in LM-treated DS mice vs. saline-treated DS mice (21.37 ± 2.01 Hz, $n = 15$ cells from 5 mice vs. 12.2 ± 1.55 Hz $n = 14$ cells from 5 mice, $P < 0.01$ by post hoc Tukey's test following one-way ANOVA) (Fig. 2 *D–F*). There was also a trend toward an increase in the frequency of mIPSCs and sIPSCs in LM-treated WT mice vs. saline-treated WT mice (mIPSC: 15.13 ± 1.87 Hz, $n = 14$ cells from 6 mice vs. 10.76 ± 1.07 Hz, $n = 21$ cells from 7 mice; sIPSC: 23.54 ± 2.15 Hz, $n = 24$ cells from 8 mice vs. 18.13 ± 1.28 Hz, $n = 19$ cells from 7 mice), although the differences were not significant (post hoc Tukey's test following one-

way ANOVA). To test whether the increased frequency of IPSCs in LM-treated DS mice was due to increased GABA release probability, we evoked monosynaptic IPSCs in layer Va Pyr cells (*Materials and Methods*). An analysis of the evoked IPSCs (eIPSCs) showed a decreased paired pulse ratio (PPR) in LM-treated (0.71 ± 0.03, $n = 13$ cells from 5 mice) vs. saline-treated DS mice (0.89 ± 0.07, $n = 16$ cells from 6 mice, $P < 0.05$ by post hoc Dunn's test following the Kruskal–Wallis test) (Fig. 2 *J–N*), indicating that LM treatment increases GABA release probability. Upregulated N and P/Q-type calcium channels in presynaptic inhibitory terminals induced by LM treatment may contribute to the increased probability of GABA release (22). The eIPSC data also suggested the contribution of

Gu et al.
Chronic partial TrkB activation reduces seizures and mortality in a mouse model of Dravet syndrome

PNAS | 3 of 8
https://doi.org/10.1073/pnas.2022726119

PV interneurons to the increased IPSCs, as the stimulating electrode was placed close to the soma of Pyr cells, presumably mainly stimulating the PV axon terminals which are the predominant inhibitory input onto the soma of Pyr cells in the neocortex (23). To determine whether LM treatment also affected excitatory synaptic transmission, spontaneous excitatory postsynaptic currents (sEPSCs) were recorded from layer Va Pyr cells. Results showed no significant changes in the frequency or amplitude of sEPSC in the LM-treated vs. saline-treated DS and WT mice (Fig. 2 G–I).

LM Treatment Upregulates Na$_v$1.1 in DS Mice. A further analysis of sIPSCs and mIPSCs on Pyr cells (Fig. 2 B and E) showed that there was a greater increase in the frequency of sIPSCs compared to mIPSCs in LM-treated DS mice (75% vs. 59%). This result is consistent with an effect of LM treatment to increase

Na$_v$1.1 and intrinsic excitability of PV interneurons that is known to be impaired in DS mice due to the loss of function of Na$_v$1.1 (7, 10). To test this hypothesis, we performed standard IHC and Western blotting to examine the Na$_v$1.1-IR and protein levels in the cortex. The IHC data showed that perisomatic Na$_v$1.1-IR around PV cells in layer Va was decreased in DS mice (DS+saline: $2.88 \pm 0.17\%$, $n = 9$ sections from 3 mice) vs. normal WT mice (WT+saline: $6.10 \pm 0.21\%$, $n = 9$ sections from 3 mice, $P < 0.01$), and LM treatment significantly enhanced perisomatic Na$_v$1.1-IR around PV cells in DS mice (DS+LM: $5.85 \pm 0.19\%$, $n = 9$ sections from 3 mice, $P < 0.05$) (Fig. 3 A–E). Perisomatic Na$_v$1.1-IR around Pyr cells was also significantly increased in LM-treated DS mice ($2.38 \pm 0.16\%$, $n = 9$ sections from 3 mice) vs. saline-treated DS mice ($1.40 \pm 0.34\%$, $n = 9$ sections from 3 mice, $P < 0.0001$ by post hoc Dunn's test following the Kruskal–Wallis test) (Fig. 3 A–F).
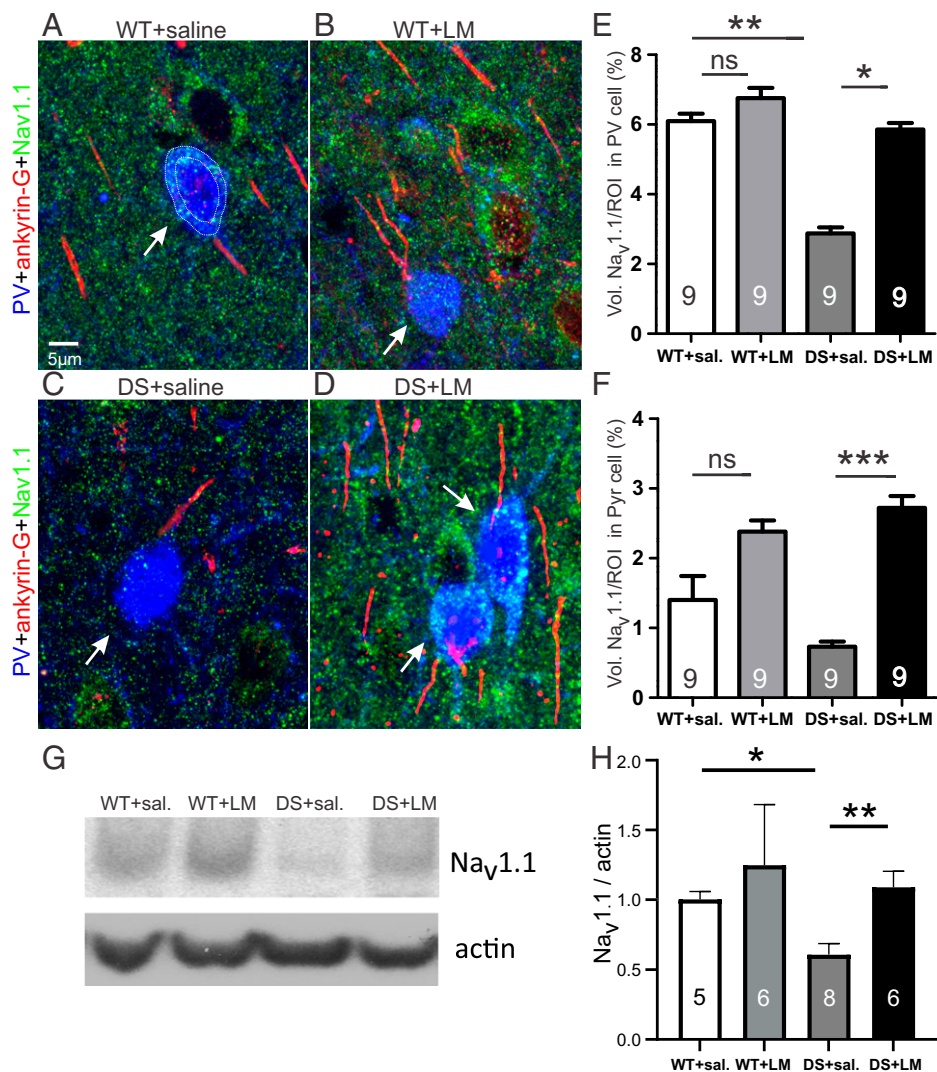

Fig. 3. LM treatment upregulates Na$_v$1.1 in DS mice. (A–D) Confocal images of triple IR for Na$_v$1.1 (green)+PV (blue)+ankyrin G (red) in layer V of cortex from saline (sal)- (A) and LM-treated WT mice (B), and saline- (C) and LM- (D) treated DS mice. Arrows point to PV cells. "Railroad track" (white dash lines) around the soma of a PV cell in A indicates perisomatic ROI. (E) The graph shows a significant decrease of Na$_v$1.1-IR in the perisomatic ROI of PV cells in DS+saline vs. WT+saline mice. LM treatment of DS mice significantly increases perisomatic Na$_v$1.1-IR. Numbers in bars: number of sections (three sections/ mouse). **$P < 0.01$; *$P < 0.05$ by post hoc Dunn's test following the Kruskal–Wallis test. (F) The graph shows a similar increase of Na$_v$1.1-IR in the perisomatic ROI of pyramidal cells in LM vs. saline-treated DS mice. Results are expressed as cumulative volume of Na$_v$1.1-IR/total volume of perisomatic ROI. Numbers in bars: number of sections (three sections/mouse). ***$P < 0.001$ by post hoc Dunn's test the following Kruskal–Wallis test. (G) Representative immunoblots of Na$_v$1.1 and actin from the cortices of saline- and LM-treated WT and DS mice. (H) OD of Na$_v$1.1 immunoblots normalized to that of actin. The graph shows decreased Na$_v$1.1 protein level in DS+saline mice vs. WT+saline mice. LM treatment significantly upregulated Na$_v$1.1 protein level in DS mice. Numbers in bars: number of mice. **$P < 0.01$; *$P < 0.05$ by post hoc Dunn's test following the Kruskal–Wallis test. ns, not significant.
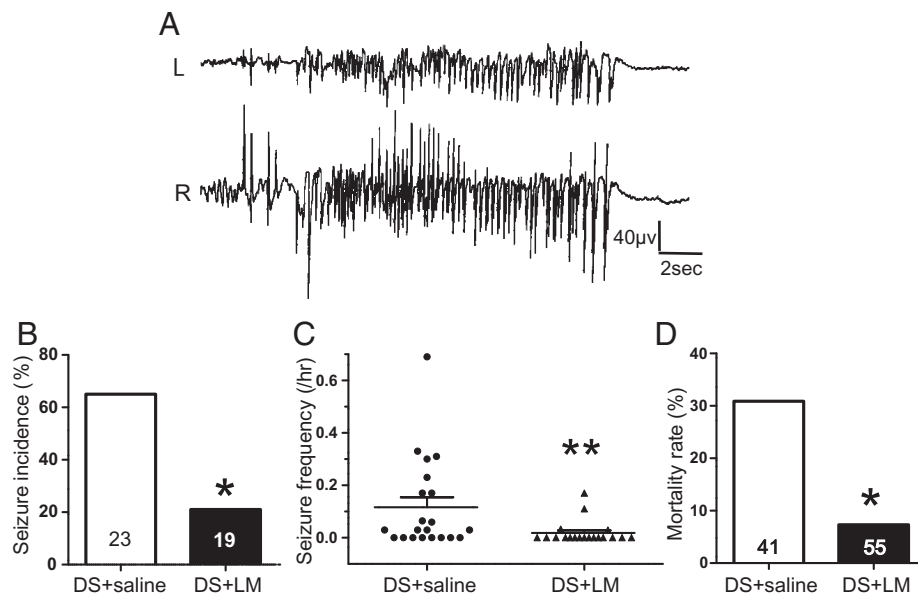
Fig. 4. LM treatment reduces seizures and mortality in DS mice. (*A*) Representative EEG recording of a spontaneous seizure in a chronically implanted DS mouse. L and R denote leads from epidural electrodes over the left and right parietal cortex, respectively. (*B* and *C*) Incidence (*B*) and frequency (*C*) of spontaneous seizures are significantly decreased in LM-treated vs. saline-treated DS mice. (*D*) LM treatment significantly decreased mortality rate from 31% (17/55) to 7% (4/31) during the first month in DS mice. Numbers in bars: number of animals. *$P < 0.05$ by χ^2 test; **$P < 0.01$ by Mann–Whitney test.

Consistent with the IHC results, the Western blot showed that the $Na_v1.1$ protein level in the cortex of DS mice (0.608 ± 0.079, $n = 8$ mice) was decreased compared with WT mice (1.003 ± 0.056, $n = 6$ mice, $P < 0.05$), and LM treatment significantly increased the $Na_v1.1$ level in DS mice (1.089 ± 0.11, $n = 6$ mice, $P < 0.05$, by post hoc Dunn's test following the Kruskal–Wallis test) (Fig. 3 *G* and *H*). The results indicate that LM treatment can increase $Na_v1.1$ expression in the cortex of DS mice.

LM Reduces Epilepsy and Mortality in DS Mice. *Scn1a* mutation and loss of function of $Na_v1.1$ lead to the impairment of PV interneuronal activity, causing frequent spontaneous seizures and high susceptibility to hyperthermia-induced seizures in DS mice (24, 25). Spontaneous seizures (*SI Appendix*, Movie S1) in our mouse model of DS start at ~P18 and occur frequently between postnatal weeks 3 and 4. We hypothesized that LM treatment would suppress spontaneous seizures in DS mice by boosting PV interneuron function and correcting the imbalance between inhibition and excitation. To test this hypothesis, spontaneous seizure incidence and frequency were assessed blindly in saline- and LM-treated DS mice. DS mice received saline or LM treatment 1×/d for 7 d beginning at P13, and video monitoring was done 2 d after the last dose, from 7 PM to 7 AM during P21 to P23, when untreated DS mice have frequent seizures. Results (Fig. 4 *A–C*) showed that spontaneous seizures (Racine class 3 or above) occurred in 65% (15/23) of saline-treated DS mice, while only 21% (4/19) of LM-treated DS mice had seizures during the P21 to P23 time interval ($P = 0.0166$, χ^2 test). Additional monitoring was also performed on 8 DS+saline and 8 DS+LM mice during a 7-d treatment from P13 to P19. Results showed that 50% (4/8) of DS+saline mice had seizures that started at P17 (1 mouse) and P19 (3 mice) respectively, while only 12.5% (1/8) of DS+LM mice had seizures that started at P19. LM treatment also significantly reduced seizure frequency in DS mice from 0.81 seizures/mouse/h (23 mice) to 0.02 seizures/mouse/h (19 mice) ($P = 0.003$, Mann–Whitney test). Consistent with previous findings (7), our results showed that 31% (17/55) of DS mice died in the first month. LM

treatment reduced the mortality rate to 7% (3/41), or a 77% reduction ($P = 0.019$, χ^2 test) (Fig. 4*D*). Together, these results show that chronic 7-d LM treatment early in life can reduce the incidence and frequency of spontaneous seizures and mortality rate in a transgenic mouse model of DS.

Discussion

The important therapeutic objective in DS is controlling the frequent seizures and associated debilitating comorbidities including sudden unexpected death in epilepsy (SUDEP). However, existing antiepileptic drugs are inadequate to suppress seizures in DS (26). Seizures can induce additional structural and functional changes in the brain that contribute to chronic epilepsy and cognitive dysfunction (27, 28). In DS, there is a strong correlation of seizures with cognitive decline and SUDEP (29, 30), emphasizing the importance of early treatment to prevent or reduce the occurrence of seizures. Based on the critical role of PV interneuronal dysfunction in the pathogenesis of DS and previous positive effects of TrkB partial agonist to enhance PV interneuron function and suppress epileptogenesis following traumatic brain injury (15), we investigated whether the same treatment with TrkB receptor partial agonist LM early in life could improve PV function and prevent seizure occurrence in a mouse model of DS with a mutation of the *Scn1a* gene that encodes $Na_v1.1$. This model carries the gene mutation identical to that found in three unrelated patients with DS and has robust spontaneous seizures, cognitive impairment, and behavioral deficits seen in DS patients (7, 24).

Our study showed that LM reaches high concentration in the whole brain tissue extract of young P16 DS mice at 0.5 h, 1 h, and 3 h after the fourth dose of treatment (90.6 μM, 98.1 μM, and 74.5 μM respectively; Absorption Systems), indicating a good blood–brain barrier penetration of LM in mammalian brain when applied intranasally and intraperitoneally early in life. Early LM treatment in DS mice resulted in increased PV synapses on Pyr cells with an increased frequency of mIPSCs, as well as increased GABA release probability, indicated by decreased PPR for monosynaptic IPSCs. The known actions of

Gu et al.
Chronic partial TrkB activation reduces seizures and mortality in a mouse model of Dravet syndrome

PNAS | 5 of 8
https://doi.org/10.1073/pnas.2022726119

BDNF to induce sprouting of axonal terminals and dendrites of inhibitory interneurons during development (31) and induce the formation of inhibitory synapses (32, 33) raise the possibility that such sprouting and inhibitory synaptogenesis may contribute to the enhanced PV synapses in the LM-treated DS mice. The increased GABA release probability in the LM-treated DS mice could be associated with the upregulated N-type and P/Q-type calcium channels in GABAergic interneuronal terminals (22, 34). Additionally, LM treatment also upregulated $Na_v1.1$, which is prominently expressed in AIS and somata of PV interneurons. The loss of $Na_v1.1$ due to the *Scn1a* mutation decreases PV interneuron function and results in epilepsy in DS mice (7, 10, 12). The upregulation of $Na_v1.1$ by LM treatment in DS mice could mitigate this abnormality in PV interneurons and further contribute to enhanced PV interneuron function. The mechanisms by which TrkB activation increases $Na_v1.1$ expression in this DS model require further study.

LM treatment also significantly reduced the seizure incidence and frequency in DS mice. Decreases in spontaneous or hyperthermia-induced seizures have also been reported in other models of DS in which $Na_v1.1$ activity and interneuronal function are enhanced with spider venom peptide Hm1a (35), using a dCas9-based *Scn1a* gene activation approach (36) or a synthesized $Na_v1.1$ activator AA43279 in zebra fish (37, 38). Recent studies have suggested that other compounds, such as recombinant Hm1b (another spider venom peptide), Hj1a, and Hj2a (scorpion venom peptides), may also have therapeutic potential for DS treatment by potentiating $Na_v1.1$ activity with varied degrees of selectivity (39, 40). The role of BDNF/TrkB signaling in epileptogenesis is controversial, with reports of both pro- (41–43) and antiepileptogenic effects (15, 44–47). These opposite results could be due to a number of factors, including effects of acute vs. chronic BDNF treatment (48, 49), opposing effects of BDNF at its TrkB and p75 receptors (50), different experimental models used, and differences in the downstream cascades activated following activation of TrkB receptors (15). LM, the small molecule used in the present study, only partially activates the TrkB receptor and its downstream pathways (16, 51) and thereby exerts antiepileptogenic effects by enhancing inhibition without affecting excitation (Fig. 2), as in earlier experiments (15). LM may exert its beneficial actions on DS through other mechanisms that were not investigated in the present study, such as its possible effects on other subtypes of interneurons or on neuroinflammation by modulating microglia activation (52).

In DS, convulsive seizures continue into adulthood and cognitive and behavioral comorbidities also appear later in life. *Scn1a* mutations and seizures may interact to increase the severity of the DS phenotype (53). Secondary changes following PV interneuron dysfunction and early frequent seizures may contribute to chronic epilepsy and later comorbidities in DS (27, 54). The early prevention of seizure occurrence by targeting PV interneurons with LM treatment may have long-term beneficial effects to decrease seizures as well as cognitive deficits.

High premature mortality is a major issue in DS patients, with a death rate ranging from 5 to 20% (55, 56). Epilepsy-related deaths due to SUDEP and status epilepticus (SE) account for the vast majority of premature mortality in DS, with SUDEP being the leading cause of death (49%), followed by fatal SE (32%) (55). The risk of SUDEP in children with DS is estimated to be 15-fold higher than in other types of childhood-onset epilepsies (51, 57). As in human DS, DS mice also have a high rate of premature death and SUDEP that peaks in the juvenile period between 3 to 5 wk of age (7). The exact mechanisms responsible for SUDEP are not known, but animal and human studies have found that the occurrence of SUDEP has a strong correlation with seizure severity and

frequency of generalized convulsive seizures (29, 58). Early treatment of DS mice with LM remarkably decreased the occurrence of convulsive seizures as well as premature mortality, indicating that LM could be an effective treatment to prevent these complications

In summary, our data provide to our knowledge the first evidence that early treatment with a small-molecule partial TrkB receptor agonist might be a promising strategy to correct the dysfunction of interneurons, the core deficit in DS, and thereby prevent seizure occurrence and premature death. Further studies are required to evaluate whether early LM treatment has long-term effects on seizures and cognitive and behavioral deficits in DS to determine which TrkB downstream pathways are involved in LM's effects presented here and the possible role of other cortical interneuronal subtypes in LM effects. The results also showed similar effects of LM on WT mice, as was also found in a previous study on posttraumatic epileptogenesis (15), suggesting that LM's effects are not specific to DS. Given that the dysfunction of PV interneurons is also critically associated with other neurological disorders, such as autism, Alzheimer's disease, and other types of epilepsies (59–61), our results may have relevance beyond DS.

Materials and Methods

All experiments were carried out according to National Institutes of Health Guide for the Care and Use of Laboratory Animals and protocols approved by the Stanford Institutional Animal Care and Use Committee.

Animals and Drug Administration. The mouse model of DS used in this study, with a loss-of-function mutation in the *Scn1a* gene (7), was developed by Kazuhiro Yamakawa at RIKEN Brain Science Institute. All DS mice used in the experiments were heterozygous (HET) *Scn1a* mutant mice with both males and females included. P13 HET DS mice were given either saline or LM (coded, 50 mg/kg intraperitoneal + 5 mg/kg intranasal once a day) for 7 d. Brain concentrations of LM with this dosage protocol were assessed by Absorption Systems (*Discussion*). IHC and Western blot experiments were performed 7 d after the end of treatment, and electrophysiological recordings were obtained 2 to 7 d after the last treatment.

Brain Slice Preparation. Mice were anesthetized, and using previously described techniques (62), brains were removed. Coronal neocortical slices (~300 μm) were cut with a vibratome in cold (4 ± 1 °C), "slicing" artificial cerebrospinal fluid (ACSF) containing (in mM) 126 NaCl, 2.5 KCl, 1.25 NaH_2PO_4, 1 $CaCl_2$, 2 $MgSO_4$, 26 $NaHCO_3$, and 10 glucose (pH 7.4) when saturated with 95% O_2/5% CO_2. Slices were then transferred to an incubation chamber filled with standard ACSF containing (in mM) 126 NaCl, 2.5 KCl, 1.25 NaH_2PO_4, 2 $CaCl_2$, 1 $MgSO_4$, 26 $NaHCO_3$, and 10 glucose. Slices were incubated at 33 ± 1 °C for 1 h and then at room temperature before use.

Whole-Cell Patch-Clamp Recording. After incubation, slices were transferred to a recording chamber where they were minimally submerged (32 ± 1 °C) and perfused at the rate of 2.5 to 3 mL/min with standard ACSF. Patch electrodes were pulled from borosilicate glass tubing (1.5 mm optical density) and had impedances of 4 to 6 MΩ when filled with a Cs-gluconate–based intracellular solution containing (in mM) 120 Cs-gluconate, 10 KCl, 11 EGTA, 1 $CaCl_2 \cdot 2 H_2O$, 2 $MgCl_2 \cdot 6H_2O$, 10 HEPES, 2 Na_2ATP, and 0.5 NaGTP. The osmolarity of the pipette solution was adjusted to 285 to 295 mOsm and the pH to 7.35 to 7.4 with CsOH. E_{Cl}^- was −70 mV calculated from the Nernst equation.

Whole-cell voltage-clamp recordings of sIPSCs were obtained from layer Va Pyr cells at a holding potential (V_h) of +20 mV without application of glutamate receptor blockers (63, 64). mIPSCs were recorded in the presence of 1 μM tetrodotoxin (TTX; Ascent Scientific). Pharmacologically isolated monosynaptic (e) IPSCs were reliably evoked with monopolar tungsten stimulating electrodes, placed in layer V, ~100 μm below the recorded Pyr soma (62). To obtain the threshold (T) for evoking IPSCs, the stimulus duration was initially set at 100 μs and stimulus intensity increased until a stable eIPSC with a failure rate of ≤50% was evoked. The pulse duration was then increased to 150 μs (1.5 × threshold; "1.5T" below), and responses to pairs of pulses with an interstimulus interval (ISI) of 50 ms, delivered at a repetition rate of 0.05 Hz, were recorded. To decrease variability, responses evoked by ≥10 pairs of stimuli were averaged. The PPR was calculated as the peak amplitude of the second eIPSC (R2) divided by the amplitude of the first eIPSC (R1).

sEPSCs were recorded from layer Va Pyr cells at $V_h = -70\text{mV}$ and the estimated E_{Cl^-} with the Cs-gluconate internal solution (64). All recordings were made with a Multiclamp 700A amplifier, sampled at 10kHz, filtered at 4kHz with a Digidata 1320A digitizer, and analyzed using Clampfit 9.0 (Molecular Devices), Mini Analysis (Synaptosoft), and Prism (GraphPad software). Only recordings with a stable access resistance of $<20\text{M}\Omega$ that varied $<15\%$ during the recording were accepted for analysis. One neuron was recorded per slice, and no more than three slices were used per mouse.

IHC and Image Analysis. Methods for IHC were as previously described (15, 65). Mice were deeply anesthetized with Beuthanasia-D (110mg/kg) and perfused transcardially with 4% paraformaldehyde. Coronal brain sections (40μm) were cut with a microtome (Microm, HM 400). Free-floating sections were incubated for 1h in 10% normal donkey serum in phosphate buffered saline (PBS), followed by a 48-h incubation with the primary antibodies against PV (mouse monoclonal anti-PV, Millipore; 1:250), gephyrin (mouse monoclonal anti-gephyrin, SySy, 1:250), VGAT (Guinea pig anti-VGAT, SySy, 1:500), $Na_v1.1$ (rabbit anti-$Na_v1.1$, Alomone [ASC-001], 1:500), synaptotagmin 2 (rabbit polyclonal anti-synaptotagmin 2, SySy, 1:100), ankyrin G (guinea pig anti-ankyrin G, SySy, 1:1,000), and NeuN (mouse anti-NeuN, Millipore, 1:100). Subsequently, sections were rinsed in PBS and incubated for 2h with the corresponding fluorescent secondary antibodies (Jackson Immuno Research Laboratories). Sections were mounted on slides using Vectashield mounting media and stored at 4 °C until visualization.

Immunofluorescence was assessed with a laser scanning confocal microscope (Zeiss 880). Confocal image stacks were obtained with 0.37-μm separation in the z axis at 63×. IMARIS 9.5.2 software was used for image analysis to detect and quantify $Na_v1.1$- IR within perisomatic ROI of the PV cell and Pyr cell; or close appositions of PV-, VGAT-, and gephyrin-IR; or close appositions of PV-, synaptotagmin 2-, and NeuN-IR (presumptive PV inhibitory synapses) within perisomatic ROI of the Pyr neuron in the layer Va cortex. The cumulative volume of $Na_v1.1$-IR, colocalized PV/VGAT/gephyrin-IR, or colocalized PV/synaptotagmin 2/NeuN-IR was expressed as a percentage of the total volume of perisomatic ROI (22). Please see more details in *SI Appendix*.

Western Blot. Fresh full-thickness cortical brain tissue was dissected and sonicated in homogenization buffer, as follows: 12.5% 0.5 M Tris·HCl, 10% glycerol, 2% SDS, and protease inhibitor mixture (Thermo Scientific). Homogenates were centrifuged at $14,000 \times g$ for 15 min at 4 °C, and the supernatant was collected. Samples of protein (15 to 20 μg) were separated by 4 to 15% Tris-HCl running gel and transferred to Amersham Hybond-P transfer membranes (GE Healthcare). Membranes were blocked with 5% nonfat milk in Tris-buffered saline with Tween (TBST) for 1 h at room temperature and incubated overnight at 4 °C with primary antibodies against $Na_v1.1$ (Alomone [ASC-001]; 1:500). After several washes, the membranes were incubated with secondary antibodies at dilutions of 1: 10,000 for 1.5 h at room temperature. After further extensive washing, the immunoreactive bands were detected with ECL plus Western blot detection system reagents (GE Healthcare). Quantification of the OD of Western blots was performed using Un-Scan-It gel software (v6.1; Silk Scientific). The relative expression of specific protein was normalized and calculated as the OD of specific protein/OD of actin.

Video/EEG Recording. Animals were anesthetized with isoflurane and implanted with epidural electrodes as previously described (66). Electrodes consisting of 0.003-inch diameter silver wires (Medwire), insulated to within ~0.5 mm of their cut ends, were presoldered to a microminiaturize connector, and ends were placed epidurally through the drill holes over the left and right parietal cortex between bregma and lambda, 2 mm from the midline. A reference electrode was implanted in the midline over the cerebellum. All mice resumed normal behavior within a few hours after surgery and were allowed to rest for at least 48 h before recordings. To acquire electroencephalography (EEG) data, the implanted plug was connected to a XLTEK 32-channel box (Natus Medical Incorporated) with a flexible cable. EEG signals were filtered using a 0.5-Hz high-pass filter, 80-Hz low-pass filter, and a 60-Hz notch filter. Seizure activities on EEG were identified as burst-like events of high amplitude containing spikes and sharp waves, corresponding to simultaneous video-recorded seizure behavior. Spontaneous seizures were assessed blindly in saline- and LM-treated DS mice that were monitored from 7 PM to 7 AM for 2 d after the last dose of LM, during P21 to P23 when DS mice have frequent seizures. High-resolution digital cameras with infrared function were connected to the PC workstation for data storage and used to record seizure behaviors. To increase efficiency, only some of the mice (5 DS+saline mice and 5 DS+LM mice) were implanted with EEG electrodes for video-EEG recordings. Other animals (18 DS+saline mice and 14 DS+LM mice) were monitored with video recordings only, the resulting video files reviewed at 8× speed, and suspected seizures assessed at real time. Seizure incidence and frequency were measured and compared between groups. Seizure incidence is defined as the percentage of mice in each group that have experienced at least one seizure during 3 d of recording from P21 to P23. Seizure severity is graded from 1 to 5 using the Racine score. Only seizures with severity of Racine scale 3 and above were included for analysis.

Statistical Analysis. Data are expressed as mean ± SEM and were analyzed using GraphPad Prism software. Statistical significance of differences was measured using one-way ANOVA followed by post hoc Tukey test, or Kruskal–Wallis followed by post hoc Dunn's test, as appropriate and as indicated in the figure legends. The Shapiro–Wilk normality test was used to determine data normality. The Mann–Whitney test was used to analyze seizure frequency, and the χ^2 test was used to analyze seizure incidence and mortality rate in DS mice. $P < 0.05$ was considered significant. Data analysis was done blindly. Sample size was determined based on pilot experiments.

Data Availability. All study data are included in the article and supporting information (*SI Appendix*, Dataset S1).

1. C. Dravet, The core Dravet syndrome phenotype. *Epilepsia* **52** (suppl. 2), 3–9 (2011).
2. P. Genton, R. Velizarova, C. Dravet, Dravet syndrome: The long-term outcome. *Epilepsia* **52** (suppl. 2), 44–49 (2011).
3. R. Nabbout *et al.*, FAiRE, DS Study Group, Fenfluramine for treatment-resistant seizures in patients with Dravet syndrome receiving stiripentol-inclusive regimens: A randomized clinical trial. *JAMA Neurol.* **77**, 300–308 (2020).
4. O. Devinsky *et al.*, Cannabidiol in Dravet Syndrome Study Group, Trial of cannabidiol for drug-resistant seizures in the Dravet syndrome. *N. Engl. J. Med.* **376**, 2011–2020 (2017).
5. A. Griffin *et al.*, Clemizole and modulators of serotonin signalling suppress seizures in Dravet syndrome. *Brain* **140**, 669–683 (2017).
6. K. Yamakawa, Molecular and cellular basis: Insights from experimental models of Dravet syndrome. *Epilepsia* **52** (suppl. 2), 70–71 (2011).
7. I. Ogiwara *et al.*, Nav1.1 localizes to axons of parvalbumin-positive inhibitory interneurons: A circuit basis for epileptic seizures in mice carrying an Scn1a gene mutation. *J. Neurosci.* **27**, 5903–5914 (2007).
8. J. C. Oakley, F. Kalume, W. A. Catterall, Insights into pathophysiology and therapy from a mouse model of Dravet syndrome. *Epilepsia* **52** (suppl. 2), 59–61 (2011).
9. S. Han *et al.*, Autistic-like behaviour in Scn1a+/- mice and rescue by enhanced GABA-mediated neurotransmission. *Nature* **489**, 385–390 (2012).
10. C. Tai, Y. Abe, R. E. Westenbroek, T. Scheuer, W. A. Catterall, Impaired excitability of somatostatin- and parvalbumin-expressing cortical interneurons in a mouse model of Dravet syndrome. *Proc. Natl. Acad. Sci. U.S.A.* **111**, E3139–E3148 (2014).
11. M. Rubinstein *et al.*, Dissecting the phenotypes of Dravet syndrome by gene deletion. *Brain* **138**, 2219–2233 (2015).
12. S. B. Dutton *et al.*, Preferential inactivation of Scn1a in parvalbumin interneurons increases seizure susceptibility. *Neurobiol. Dis.* **49**, 211–220 (2013).
13. T. Tatsukawa, I. Ogiwara, E. Mazaki, A. Shimohata, K. Yamakawa, Impairments in social novelty recognition and spatial memory in mice with conditional deletion of Scn1a in parvalbumin-expressing cells. *Neurobiol. Dis.* **112**, 24–34 (2018).
14. J. C. Oakley, A. R. Cho, C. S. Cheah, T. Scheuer, W. A. Catterall, Synergistic GABA-enhancing therapy against seizures in a mouse model of Dravet syndrome. *J. Pharmacol. Exp. Ther.* **345**, 215–224 (2013).
15. F. Gu, I. Parada, T. Yang, F. M. Longo, D. A. Prince, Partial TrkB receptor activation suppresses cortical epileptogenesis through actions on parvalbumin interneurons. *Neurobiol. Dis.* **113**, 45–58 (2018).
16. S. M. Massa *et al.*, Small molecule BDNF mimetics activate TrkB signaling and prevent neuronal degeneration in rodents. *J. Clin. Invest.* **120**, 1774–1785 (2010).
17. F. M. Longo, S. M. Massa, Small-molecule modulation of neurotrophin receptors: A strategy for the treatment of neurological disease. *Nat. Rev. Drug Discov.* **12**, 507–525 (2013).
18. F. Han *et al.*, Delayed administration of a small molecule tropomyosin-related kinase B ligand promotes recovery after hypoxic-ischemic stroke. *Stroke* **43**, 1918–1924 (2012).
19. D. A. Schmid *et al.*, A TrkB small molecule partial agonist rescues TrkB phosphorylation deficits and improves respiratory function in a mouse model of Rett syndrome. *J. Neurosci.* **32**, 1803–1810 (2012).
20. D. A. Simmons *et al.*, A small molecule TrkB ligand reduces motor impairment and neuropathology in R6/2 and BACHD mouse models of Huntington's disease. *J. Neurosci.* **33**, 18712–18727 (2013).
21. E. Favuzzi *et al.*, Distinct molecular programs regulate synapse specificity in cortical inhibitory circuits. *Science* **363**, 413–417 (2019).
22. F. Gu, I. Parada, T. Yang, F. M. Longo, D. A. Prince, Partial activation of TrkB receptors corrects interneuronal calcium channel dysfunction and reduces epileptogenic activity in neocortex following injury. *Cereb. Cortex* **30**, 5180–5189 (2020).

Gu et al.
Chronic partial TrkB activation reduces seizures and mortality in a mouse model of Dravet syndrome

PNAS | 7 of 8
https://doi.org/10.1073/pnas.2022726119

23. R. Tremblay, S. Lee, B. Rudy, GABAergic interneurons in the neocortex: From cellular properties to circuits. *Neuron* **91**, 260–292 (2016).

24. D. Cao *et al.*, Efficacy of stiripentol in hyperthermia-induced seizures in a mouse model of Dravet syndrome. *Epilepsia* **53**, 1140–1145 (2012).

25. J. C. Oakley, F. Kalume, F. H. Yu, T. Scheuer, W. A. Catterall, Temperature- and age-dependent seizures in a mouse model of severe myoclonic epilepsy in infancy. *Proc. Natl. Acad. Sci. U.S.A.* **106**, 3994–3999 (2009).

26. J. H. Cross *et al.*, Dravet syndrome: Treatment options and management of prolonged seizures. *Epilepsia* **60** (suppl. 3), S39–S48 (2019).

27. G. L. Holmes, Cognitive impairment in epilepsy: The role of network abnormalities. *Epileptic Disord.* **17**, 101–116 (2015).

28. J. Chin, H. E. Scharfman, Shared cognitive and behavioral impairments in epilepsy and Alzheimer's disease and potential underlying mechanisms. *Epilepsy Behav.* **26**, 343–351 (2013).

29. C. Harden *et al.*, Practice guideline summary: Sudden unexpected death in epilepsy incidence rates and risk factors: Report of the guideline development, dissemination, and implementation Subcommittee of the American Academy of Neurology and the American Epilepsy Society. *Neurology* **88**, 1674–1680 (2017).

30. L. Lagae, I. Brambilla, A. Mingorance, A. Gibson, A. Battersby, Quality of life and comorbidities associated with Dravet syndrome severity: A multinational cohort survey. *Dev. Med. Child Neurol.* **60**, 63–72 (2018).

31. X. Jin, H. Hu, P. H. Mathers, A. Agmon, Brain-derived neurotrophic factor mediates activity-dependent dendritic growth in nonpyramidal neocortical interneurons in developing organotypic cultures. *J. Neurosci.* **23**, 5662–5673 (2003).

32. M. R. Palizvan *et al.*, Brain-derived neurotrophic factor increases inhibitory synapses, revealed in solitary neurons cultured from rat visual cortex. *Neuroscience* **126**, 955–966 (2004).

33. B. Rico, B. Xu, L. F. Reichardt, TrkB receptor signaling is required for establishment of GABAergic synapses in the cerebellum. *Nat. Neurosci.* **5**, 225–233 (2002).

34. P. Baldelli, J. M. Hernandez-Guijo, V. Carabelli, E. Carbone, Brain-derived neurotrophic factor enhances GABA release probability and nonuniform distribution of N- and P/Q-type channels on release sites of hippocampal inhibitory synapses. *J. Neurosci.* **25**, 3358–3368 (2005).

35. K. L. Richards *et al.*, Selective Na$_v$1.1 activation rescues Dravet syndrome mice from seizures and premature death. *Proc. Natl. Acad. Sci. U.S.A.* **115**, E8077–E8085 (2018).

36. G. Colasante *et al.*, dCas9-based Scn1a gene activation restores inhibitory interneuron excitability and attenuates seizures in Dravet syndrome mice. *Mol. Ther.* **28**, 235–253 (2020).

37. W. J. Weuring *et al.*, NaV1.1 and NaV1.6 selective compounds reduce the behavior phenotype and epileptiform activity in a novel zebrafish model for Dravet syndrome. *PLoS One* **15**, e0219106 (2020).

38. K. Frederiksen *et al.*, A small molecule activator of Na$_v$ 1.1 channels increases fast-spiking interneuron excitability and GABAergic transmission in vitro and has anticonvulsive effects in vivo. *Eur. J. Neurosci.* **46**, 1887–1896 (2017).

39. C. Y. Chow *et al.*, Venom peptides with dual modulatory activity on the voltage-gated sodium channel Na$_v$1.1 provide novel leads for development of antiepileptic drugs. *ACS Pharmacol. Transl. Sci.* **3**, 119–134 (2019).

40. C. Y. Chow *et al.*, A selective Na$_v$1.1 activator with potential for treatment of Dravet syndrome epilepsy. *Biochem. Pharmacol.* **181**, 113991 (2020).

41. S. D. Croll *et al.*, Brain-derived neurotrophic factor transgenic mice exhibit passive avoidance deficits, increased seizure severity and in vitro hyperexcitability in the hippocampus and entorhinal cortex. *Neuroscience* **93**, 1491–1506 (1999).

42. B. Gu *et al.*, A peptide uncoupling BDNF receptor TrkB from phospholipase Cγ1 prevents epilepsy induced by status epilepticus. *Neuron* **88**, 484–491 (2015).

43. M. Kokaia *et al.*, Suppressed epileptogenesis in BDNF mutant mice. *Exp. Neurol.* **133**, 215–224 (1995).

44. Z. Cai *et al.*, Antagonist targeting microRNA-155 protects against lithium-pilocarpine-induced status epilepticus in C57BL/6 mice by activating brain-derived neurotrophic factor. *Front. Pharmacol.* **7**, 129 (2016).

45. B. Paradiso *et al.*, Localized delivery of fibroblast growth factor-2 and brain-derived neurotrophic factor reduces spontaneous seizures in an epilepsy model. *Proc. Natl. Acad. Sci. U.S.A.* **106**, 7191–7196 (2009).

46. D. A. Prince, F. Gu, I. Parada, Antiepileptogenic repair of excitatory and inhibitory synaptic connectivity after neocortical trauma. *Prog. Brain Res.* **226**, 209–227 (2016).

47. C. Falcicchia *et al.*, Seizure-suppressant and neuroprotective effects of encapsulated BDNF-producing cells in a rat model of temporal lobe epilepsy. *Mol. Ther. Methods Clin. Dev.* **9**, 211–224 (2018).

48. W. J. Zhu, S. N. Roper, Brain-derived neurotrophic factor enhances fast excitatory synaptic transmission in human epileptic dentate gyrus. *Ann. Neurol.* **50**, 188–194 (2001).

49. M. K. Yamada *et al.*, Brain-derived neurotrophic factor promotes the maturation of GABAergic mechanisms in cultured hippocampal neurons. *J. Neurosci.* **22**, 7580–7585 (2002).

50. C. A. Chapleau, L. Pozzo-Miller, Divergent roles of p75NTR and Trk receptors in BDNF's effects on dendritic spine density and morphology. *Neural Plast.* **2012**, 578057 (2012).

51. P. A. Kipnis, B. J. Sullivan, B. M. Carter, S. D. Kadam, TrkB agonists prevent postischemic emergence of refractory neonatal seizures in mice. *JCI Insight* **5**, e136007 (2020).

52. S. Y. Wu *et al.*, BDNF reverses aging-related microglial activation. *J. Neuroinflammation* **17**, 210 (2020).

53. A. R. Salgueiro-Pereira *et al.*, A two-hit story: Seizures and genetic mutation interaction sets phenotype severity in SCN1A epilepsies. *Neurobiol. Dis.* **125**, 31–44 (2019).

54. M. Favero, N. P. Sotuyo, E. Lopez, J. A. Kearney, E. M. Goldberg, A transient developmental window of fast-spiking interneuron dysfunction in a mouse model of Dravet syndrome. *J. Neurosci.* **38**, 7912–7927 (2018).

55. M. S. Cooper *et al.*, Mortality in Dravet syndrome. *Epilepsy Res.* **128**, 43–47 (2016).

56. M. Sakauchi *et al.*, Mortality in Dravet syndrome: Search for risk factors in Japanese patients. *Epilepsia* **52** (suppl. 2), 50–54 (2011).

57. J. V. Skluzacek, K. P. Watts, O. Parsy, B. Wical, P. Camfield, Dravet syndrome and parent associations: The IDEA League experience with comorbid conditions, mortality, management, adaptation, and grief. *Epilepsia* **52** (suppl. 2), 95–101 (2011).

58. F. Kalume *et al.*, Sudden unexpected death in a mouse model of Dravet syndrome. *J. Clin. Invest.* **123**, 1798–1808 (2013).

59. A. Maheshwari, W. K. Nahm, J. L. Noebels, Paradoxical proepileptic response to NMDA receptor blockade linked to cortical interneuron defect in stargazer mice. *Front. Cell. Neurosci.* **7**, 156 (2013).

60. E. Rossignol, Genetics and function of neocortical GABAergic interneurons in neurodevelopmental disorders. *Neural Plast.* **2011**, 649325 (2011).

61. A. Y. Lopez *et al.*, Ankyrin-G isoform imbalance and interneuronopathy link epilepsy and bipolar disorder. *Mol. Psychiatry* **22**, 1464–1472 (2017).

62. L. C. Faria, D. A. Prince, Presynaptic inhibitory terminals are functionally abnormal in a rat model of posttraumatic epilepsy. *J. Neurophysiol.* **104**, 280–290 (2010).

63. X. Jin, D. A. Prince, Excitatory and inhibitory synaptic connectivity to layer V fast-spiking interneurons in the freeze lesion model of cortical microgyria. *J. Neurophysiol.* **112**, 1703–1713 (2014).

64. X. Jin, J. R. Huguenard, D. A. Prince, Reorganization of inhibitory synaptic circuits in rodent chronically injured epileptogenic neocortex. *Cereb. Cortex* **21**, 1094–1104 (2011).

65. F. Gu *et al.*, Structural alterations in fast-spiking GABAergic interneurons in a model of posttraumatic neocortical epileptogenesis. *Neurobiol. Dis.* **108**, 100–114 (2017).

66. L. C. Faria *et al.*, Epileptiform activity and behavioral arrests in mice overexpressing the calcium channel subunit α2δ-1. *Neurobiol. Dis.* **102**, 70–80 (2017).